J. Phys. Chem. A **2008,** *112,* 4815–4825

A Density Functional Theory Study of the Structure and Vibrational Spectra of β-Carotene, Capsanthin, and Capsorubin

A. Requena,*,† J. P. Cerón-Carrasco,† A. Bastida,† J. Zúñiga,*,† and B. Miguel‡

Departamento de Química Física, Universidad de Murcia, 30100 Murcia, Spain, and Departamento de Ingeniería Química y Ambiental, Universidad Politécnica de Cartagena, 30203 Cartagena, Spain

Received: October 25, 2007; Revised Manuscript Received: March 6, 2008

A theoretical study of the structure and the vibrational spectra of the β-carotene molecule and its derivatives capsanthin and capsorubin is carried out. We first investigate systematically the theoretical method which provides the best results for β-carotene by performing ab initio calculations at the HF/6-31G(d), SVWN/6-31G(d), PBE0/6-31G(d), BLYP/6-31G(d), B3LYP/6-31G(d), B3LYP/6-31G(d,p), B3LYP/6-311G(d), and B3LYP/6-311G(d,p) levels and by using previous theoretical results available in the literature obtained at the AM1 and BPW91/6-31G(d) levels. The influence of both the level of calculation and the size of the basis set used in the geometry optimization and in the determination of the IR and Raman spectra of this molecule is thus analyzed. It is confirmed that the hybrid functional B3LYP with the basis 6-31G(d) is the method that gives the best results as a whole. By use of this level of calculation, we next optimize the molecular geometries of related molecules of capsanthin and capsorubin, which to the best of our knowledge have only been studied at the semiempirical AM1 level. In addition we calculate the IR and Raman spectra of these molecules at the B3LYP/6-31G(d) level of theory. The results obtained for capsanthin show on the one hand that the double bond of the β-ionone ring is outside the polyene chain plane, due to the repulsion between the hydrogen atoms of the ring methyl groups and the hydrogen atoms of the polyene chain, and on the other hand that the carbonyl double bond in the other headgroup is very close to planarity with the polyene chain, since in this case such a repulsion does not exist. For the molecule of capsorubin the two carbonyl groups also take the same coplanar orientation relative to the polyene chain. The IR and Raman spectra theoretically computed for these two molecules are finally compared with their experimental spectra and the vibrational normal modes of the main signals are interpreted.

I. Introduction

Carotenoids are the most abundant group of natural pigments, with more than 600 different types,[1] all derived from the same basic structure of 40 carbon atoms resulting from the polymerization of 8 units of isoprene. According to their composition, carotenoids are divided in two groups, carotenes, when they have only carbon and hydrogen atoms, and xanthophylls, when they have oxygen atoms as well. These pigments play a crucial role in the protection of cells and biological tissues against photo-oxidation processes because of their chemical ability to scavenge reactive oxygen species and free radicals.[2–5] The incorporation of carotenoids to the diet can therefore be of use in protection from oxidation damage,[6–10] and some studies have been reported that relate an increase in the consumption of carotenoids to a reduction in the risk of suffering some types of cancer or other diseases.[11–14] Capsanthin and capsorubin are two carotenoids used as colorants that are extracted from the paprika oleoresin and are responsible for the bright red color of this product[15–18] and like other carotenoids have a large antioxidant capability,[19–21] which has been related to a high antitumoral power.[22,23]

The antioxidant power of carotenoids have attracted increased attention, and this in turn has propitiated the realization of different theoretical studies in order to elucidate the molecular properties of these pigments.[24–32] Their large molecular size, of about 100 atoms, has restricted many of these studies to semiempirical treatments. The AM1 (Austin Model 1) method[33] has been used in this sense to study the geometry,[24] the electronic structure,[25] and the charge delocalization[26,27] of ionized carotenoids and also, recently, to analyze their spectroscopic properties.[28] Soffers et al.[34] have, moreover, used the PM3 semiempirical method[35,36] to determine the ionization potential of these pigments theoretically.

The methods based on the density functional theory (DFT) for electronic calculations constitute an ever-growing alternative tool to both the semiempirical and the purely ab initio and perturbative methods, mostly for molecules of large size.[37] In this context a number of DFT studies have been made recently on the β-carotene molecule.[29–32] These studies include the calculations reported by Himo[29] and by Gao et. al[32] of the electronic properties of the β-carotene radical cation using different density functionals and those conducted by Schlücker[30] and by Berezin[31] to optimize the molecular structure and to determine the IR and Raman spectra of β-carotene at the BPW91/6-31G(d) and B3LYP/6-31G(d) levels, respectively. To our knowledge, however, no study has been made to compare the performance of different DFT electronic methods when dealing with this molecule, so there is no clear evidence as to which are the best choices for both the density functional and the basis set to be used in this respect. The use of the Hartree–Fock levels of calculation for carotenoids has not been described either. Finally, no theoretical calculations at a level

---

* To whom correspondence should be addressed. E-mail: rqna@um.es (A.R.); zuniga@um.es (J.Z.).

† Universidad de Murcia.

‡ Universidad Politécnica de Cartagena.

10.1021/jp710304u CCC: $40.75

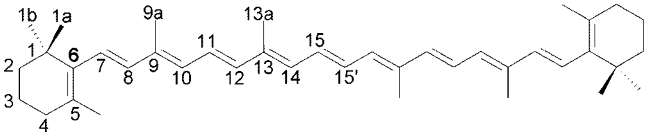

Figure 1. Molecular structure and atom numbering of β-carotene.

TABLE 1: rms Deviations of the Equilibrium Geometries of β-Carotene, as Calculated Using Different Theoretical Methods, with Respect to the Experimental Geometry (Bond Lengths Are in Angstroms, and Bond Angles Are in Degrees)

method	rms lengths	rms angles
AM1[a]	0.078	2.2
HF/6-31G(d)[b]	0.020	1.9
BLYP/6-31G(d)[b]	0.025	2.2
BPW91/6-31G(d)[c]	0.023	1.6
SVWN/6-31G(d)[b]	0.020	1.4
PBE0/6-31G(d)[b]	0.010	1.4
B3LYP/6-31G(d)[b]	0.014	1.8
B3LYP/6-31G(d,p)[b]	0.014	1.7
B3LYP/6-311G(d)[b]	0.013	1.8
B3LYP/6-311G(d,p)[b]	0.018	1.7

[a] From ref 28. [b] Present work. [c] From ref 30.

superior to the semiempirical AM1[27] have been reported for the closely related molecules of capsanthin and capsorubin.

The general objective of this work has been, therefore, to contribute to establishing a methodology to optimize the geometry and to determine the vibrational spectrum of carotenoids. To do this, we have carried out first optimization calculations for the molecule of β-carotene at the Hartree−Fock,[38] SVWN,[39] PBE0,[40] and BLYP[41,42] levels using the 6-31G(d) basis set and at the hybrid B3LYP functional level[42,43] with the basis sets 6-31G(d), 6-31G(d,p), 6-311G(d), and 6-311G(d,p). The results thus obtained, together with those taken from the literature at the AM1[28] and the BPW91/6-31G(d)[30] levels, have been used to compare the geometries optimized at all these levels with the experimental geometry determined by Senge et. al[44] from X-ray diffraction. The aim here was to investigate the performance of three different types of density functionals, namely, the SVWN (local density approximation), BLYP, BPW91 (generalized gradient approximation), PBE0, and B3LYP (hybrid) functionals, which have been found to correctly reproduce properties of related molecules,[45,30,46,47,32] in addition to the HF and AM1 approximations. We have also computed the IR and Raman spectra of the β-carotene molecule, again at all these levels, and evaluated the quality of the results obtained by comparison of the theoretical frequencies obtained for the most intense signals of these spectra with the experimental ones. From these analyses, we have concluded that the B3LYP/6-31G(d) level of calculation is that which provides the best results for the molecular structure and the vibrational spectrum of β-carotene as compared with the experiment.

Our second objective was to carry out a theoretical study of the capsanthin and capsorubin molecules for the first time at a level superior to the semiempirical, in particular by computing the geometries and the IR and Raman spectra of these two molecules using the B3LYP/6-31G(d) method, which provides the best results for β-carotene. By use of the optimized geometries thus obtained, we have analyzed how the functional groups located at both ends of the polyene chains affect their conjugation degrees. We have also compared the IR and Raman vibrational frequencies computed with those experimentally observed by Lóránd[48] and Schulz,[49] respectively, and assigned the normal modes corresponding to the main signals of the spectra.

II. Theoretical Methods

The molecule of the β-carotene has been studied using the Hartree−Fock method and the SVWN, PBE0, and BLYP functionals, all of them with a 6-31G(d) basis, and the B3LYP functional with the basis sets 6-31G(d), 6-31G(d,p), 6-311G(d), and 6-311G(d,p) which combine double- and triple-ζ functions with polarization functions on the heavy and hydrogen atoms. This choice of calculation methods has two aims, which are first to investigate the effects of the electronic correlation and second to analyze the influence of the size of the basis sets employed on both the geometry optimization and the calculation of the vibrational frequencies of the molecule. We have not considered the use of diffuse functions to describe the atomic orbitals because previous studies have shown that these functions do not improve the results for neutral molecules.[50]

To determine the effect of the electronic correlation on the β-carotene calculations, we have compared the results obtained by Weesie et al.[3] at the AM1 level using the minimum standard Slater-type basis set with our results at the Hartree−Fock and the SVWN, PBE0, BLYP, and B3LYP levels and with those

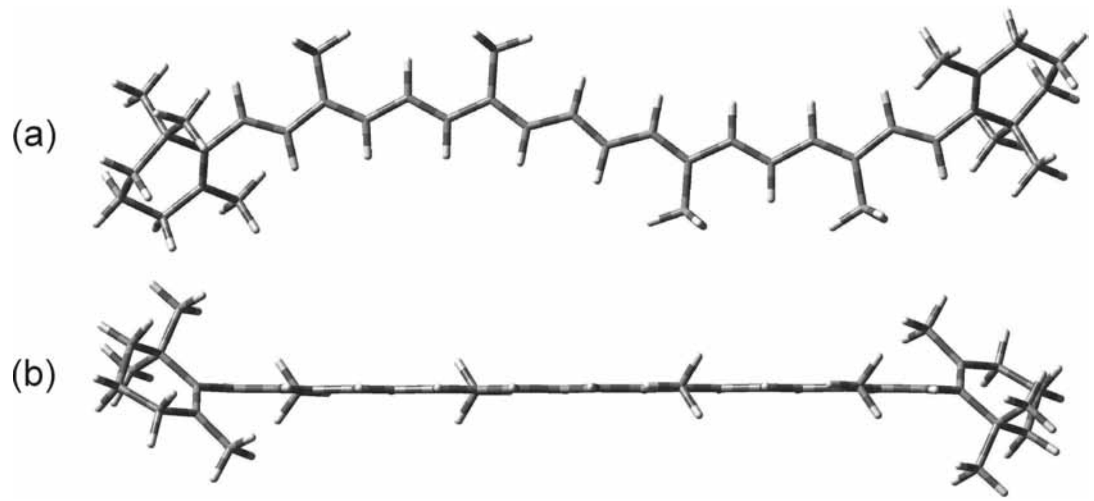

Figure 2. Molecular structure of β-carotene optimized at the B3LYP/6-31G(d) level. Normal (a) and lateral (b) views.

TABLE 2: Experimental and Calculated Bond Lengths (in Ångstroms) of β-Carotene (Δ_{len} Is the Difference between Calculated and Experimental Lengths)

		AM1[b]		HF/6-31G(d)[c]		SVWN/6-31G(d)[c]		PBE0/6-31G(d)[c]	
	exptl[a]	calcd	Δ_{len}	calcd	Δ_{len}	calcd	Δ_{len}	calcd	.Δ_{len}
$C_1{-}C_{1A}$	1.529			1.541	0.012	1.524	−0.005	1.538	0.009
$C_1{-}C_{1B}$	1.528			1.541	0.013	1.523	−0.005	1.537	0.009
$C_1{-}C_2$	1.529			1.540	0.011	1.525	−0.004	1.537	0.008
$C_1{-}C_6$	1.531	1.511	−0.020	1.542	0.011	1.524	−0.007	1.537	0.006
$C_2{-}C_3$	1.526	1.510	−0.016	1.522	−0.004	1.508	−0.018	1.519	−0.007
$C_3{-}C_4$	1.526	1.512	−0.014	1.523	−0.003	1.509	−0.017	1.520	−0.006
$C_4{-}C_5$	1.523	1.491	−0.032	1.516	−0.007	1.492	−0.031	1.507	−0.016
$C_5{-}C_{5A}$	1.502			1.512	0.010	1.487	−0.015	1.503	0.001
$C_5{=}C_6$	1.351	1.651	0.300	1.333	0.018	1.363	0.012	1.355	0.004
$C_6{-}C_7$	1.449	1.459	0.010	1.492	0.043	1.444	−0.005	1.469	0.020
$C_7{=}C_8$	1.352	1.343	−0.009	1.328	−0.024	1.361	0.009	1.352	0.000
$C_8{-}C_9$	1.445	1.457	0.012	1.474	0.029	1.428	−0.017	1.450	0.005
$C_9{-}C_{9A}$	1.500			1.509	0.009	1.488	−0.012	1.501	0.001
$C_9{=}C_{10}$	1.352	1.353	0.001	1.338	−0.014	1.374	0.022	1.365	0.013
$C_{10}{-}C_{11}$	1.442	1.443	0.001	1.459	0.017	1.410	−0.032	1.432	−0.010
$C_{11}{=}C_{12}$	1.352	1.347	−0.005	1.334	−0.018	1.370	0.018	1.361	0.009
$C_{12}{-}C_{13}$	1.444	1.455	0.011	1.468	0.024	1.417	−0.027	1.440	−0.004
$C_{13}{-}C_{13A}$	1.500			1.509	0.009	1.489	−0.011	1.502	0.002
$C_{13}{=}C_{14}$	1.353	1.354	0.001	1.340	−0.013	1.380	0.027	1.370	0.017
$C_{14}{-}C_{15}$	1.441	1.441	0.000	1.456	0.015	1.404	−0.037	1.430	−0.011
$C_{15}{=}C_{15'}$	1.346	1.350	0.004	1.335	−0.011	1.374	0.028	1.365	0.019

[a] From ref 44. [b] From ref 28. [c] Present work.

TABLE 3: Experimental and Calculated Bond Lengths (in Ångstroms) of -Carotene Including the Wiberg Bond Indices for the B3LYP/6-31Gd(d)-Optimized Geometry (Δ_{len} Is the Difference between Calculated and Experimental Lengths)

		BLYP/6-31G(d)[b]		BPW91/6-31G(d)[c]		B3LYP/6-31G(d)[b]		
	exptl[a]	calcd	Δ_{len}	calcd	Δ_{len}	calcd	Δ_{len}	Wiberg index
$C_1{-}C_{1A}$	1.529	1.561	0.032	1.551	0.022	1.546	0.017	0.9857
$C_1{-}C_{1B}$	1.528	1.560	0.032	1.552	0.024	1.549	0.021	0.9922
$C_1{-}C_2$	1.529	1.560	0.031	1.555	0.026	1.546	0.017	0.9840
$C_1{-}C_6$	1.531	1.563	0.032	1.553	0.022	1.549	0.018	0.9660
$C_2{-}C_3$	1.526	1.537	0.011	1.529	0.003	1.526	0.000	1.0131
$C_3{-}C_4$	1.526	1.539	0.013	1.531	0.005	1.529	0.003	1.0111
$C_4{-}C_5$	1.523	1.525	0.002	1.517	−0.006	1.518	−0.005	1.0175
$C_5{-}C_{5A}$	1.502	1.521	0.019	1.513	0.011	1.511	0.009	1.0340
$C_5{=}C_6$	1.351	1.373	0.022	1.371	0.020	1.358	0.007	1.7623
$C_6{-}C_7$	1.449	1.477	0.028	1.471	0.022	1.475	0.026	1.0813
$C_7{=}C_8$	1.352	1.372	0.020	1.370	0.018	1.355	0.003	1.7305
$C_8{-}C_9$	1.445	1.454	0.009	1.449	0.004	1.454	0.009	1.1560
$C_9{-}C_{9A}$	1.500	1.520	0.020	1.512	0.012	1.509	0.009	1.0250
$C_9{=}C_{10}$	1.352	1.388	0.036	1.386	0.034	1.369	0.017	1.6188
$C_{10}{-}C_{11}$	1.442	1.433	−0.009	1.429	−0.013	1.435	−0.007	1.2088
$C_{11}{=}C_{12}$	1.352	1.384	0.032	1.382	0.030	1.364	0.012	1.6305
$C_{12}{-}C_{13}$	1.444	1.441	−0.003	1.437	−0.007	1.443	−0.001	1.1960
$C_{13}{-}C_{13A}$	1.500	1.521	0.021	1.514	0.014	1.510	0.010	1.0236
$C_{13}{=}C_{14}$	1.353	1.394	0.041	1.392	0.039	1.374	0.021	1.5780
$C_{14}{-}C_{15}$	1.441	1.426	−0.015	1.422	−0.019	1.429	−0.012	1.2331
$C_{15}{=}C_{15'}$	1.346	1.388	0.042	1.386	0.040	1.369	0.021	1.6053

[a] From ref 44. [b] Present work. [c] From ref 30.

carried out by Schlucker et al.[2] at the BPW91 level. These calculations have all been performed using the same basis set 6-31G(d) as employed in previous DFT studies of carotenoids and related compounds.[30,31,51,52] The influence of the size of the basis set has been investigated in turn by carrying out calculations with the hybrid B3LYP density functional and the basis sets previously indicated. The choice of this functional is justified by the good results that it provides for the structure and the vibrational spectra of the molecule. After completing this thorough study of the β-carotene molecule, we optimized the geometries and computed the vibrational spectra of the two related molecules of capsanthin and capsorubin using the B3LYP/6-31G(d) method, which provides the best results for β-carotene.

All the calculations were made for the molecules in their neutral form and omitting the solvent effects. The molecules were also considered to have closed-shell electronic structures, so the calculations were spin restricted. The symmetry of the molecules was not constrained to the C_i point group, as it was by Schlücker et al.[30] and by Berezin et. al[31] for β-carotene, so as to ascertain whether the optimization leads to a minimum with a different symmetry or not.

The sequence of calculations was basically the same for the three molecules. We first build up the starting geometries of the molecules from their chemical structures[53] and then proceed to carry out the optimization of the geometries using the different theoretical methods described above. The bond-order Wiberg indices are also calculated in order to analyze the

TABLE 4: Experimental and Calculated Bond Angles (in Degrees) of β-Carotene (Δ_{ang} Is the Difference between Calculated and Experimental Angles)

		AM1[b]		HF/6-31G(d)[c]		SVWN/6-31G(d)[c]		PBE0/6-31G(d)[c]	
	exptl[a]	calcd	Δ_{ang}	calcd	Δ_{ang}	calcd	Δ_{ang}	calcd	$\Delta_{ang.}$
$C_1-C_2-C_3$	112.9			112.8	−0.1	112.3	−0.6	112.7	−0.2
$C_2-C_3-C_4$	104.0	110.9	6.9	109.4	5.4	108.7	4.7	109.1	5.1
$C_3-C_4-C_5$	114.4	113.5	−0.9	113.7	−0.7	113.7	−0.7	113.6	−0.8
$C_4-C_5=C_6$	121.5	122.9	1.4	123.0	1.5	122.6	1.1	122.7	1.2
$C_{5A}-C_5=C_6$	125.9			124.7	−1.2	124.2	−1.7	124.5	−1.4
$C_1-C_6=C_5$	122.1	122.9	0.8	123.0	0.9	121.8	−0.3	122.5	0.4
$C_5=C_6-C_7$	122.2	123.0	0.8	121.2	−1.0	123.1	0.9	122.4	0.2
$C_6-C_7=C_8$	126.7	124.7	−2.0	124.6	−2.1	127.6	0.9	125.5	−1.2
$C_7=C_8-C_9$	127.2	124.7	−2.5	126.5	−0.7	124.8	−2.4	126.1	−1.1
$C_8-C_9=C_{10}$	119.1	119.0	−0.1	118.0	−1.1	118.6	−0.5	118.2	−0.9
$C_{9A}-C_9=C_{10}$	122.2			124.4	2.2	122.8	0.6	123.6	1.4
$C_9=C_{10}-C_{11}$	127.3	126.1	−1.2	128.3	1.0	127.7	0.4	128.2	0.9
$C_{10}-C_{11}=C_{12}$	123.0	122.2	−0.8	122.4	−0.6	123.2	0.2	122.8	−0.2
$C_{11}=C_{12}-C_{13}$	126.1	124.9	−1.2	126.6	0.5	125.7	−0.4	126.4	0.3
$C_{12}-C_{13}=C_{14}$	117.7	118.9	1.2	118.0	0.3	118.7	1.0	118.3	0.6
$C_{13a}-C_{13}=C_{14}$	122.9			124.3	1.4	122.6	−0.3	123.3	0.4
$C_{13}=C_{14}-C_{15}$	127.7	126.4	−1.3	128.2	0.5	127.6	−0.1	128.1	0.4
$C_{14}-C_{15}=C_{15'}$	123.0	122.4	−0.6	123.0	0.0	123.7	0.7	123.4	0.4

[a] From ref 44. [b] From ref 28. [c] Present work.

TABLE 5: Experimental and Calculated Bond Angles (in Degrees) of β-Carotene (Δ_{ang} Is the Difference between Calculated and Experimental Angles)

		BLYP/6-31G(d)[b]		BPW91/6-31G(d)[c]		B3LYP/6-31G(d)[b]	
	exptl[a]	calcd	Δ_{ang}	calcd	Δ_{ang}	calcd	Δ_{ang}
$C_1-C_2-C_3$	112.9	112.8	−0.1	119.9	7.0	112.9	0.0
$C_2-C_3-C_4$	104.0	109.1	5.1	109.0	5.0	109.7	5.7
$C_3-C_4-C_5$	114.4	113.8	−0.6	113.8	−0.6	114.2	−0.2
$C_4-C_5=C_6$	121.5	122.8	1.3	122.7	1.2	122.7	1.2
$C_{5A}-C_5=C_6$	125.9	124.5	−1.4	124.4	−1.5	124.3	−1.6
$C_1-C_6=C_5$	122.1	114.9	−7.2	122.1	0.0	122.5	0.4
$C_5=C_6-C_7$	122.2	122.9	0.7	122.8	0.6	123.2	1.0
$C_6-C_7=C_8$	126.7	126.5	−0.2	126.4	−0.3	126.7	0.0
$C_7=C_8-C_9$	127.2	126.4	−0.8	126.3	−0.9	126.3	−0.9
$C_8-C_9=C_{10}$	119.1	118.3	−0.8	118.2	−0.9	118.2	−0.9
$C_{9A}-C_9=C_{10}$	122.2	123.0	0.8	123.1	0.9	123.4	1.2
$C_9=C_{10}-C_{11}$	127.3	128.6	1.3	128.4	1.1	128.4	1.1
$C_{10}-C_{11}=C_{12}$	123.0	123.1	0.1	123.1	0.1	123.0	0.0
$C_{11}=C_{12}-C_{13}$	126.1	126.9	0.8	126.7	0.6	126.7	0.6
$C_{12}-C_{13}=C_{14}$	117.7	118.4	0.7	118.3	0.6	118.3	0.6
$C_{13a}-C_{13}=C_{14}$	122.9	122.7	−0.2	122.8	−0.1	123.2	0.3
$C_{13}=C_{14}-C_{15}$	127.7	128.5	0.8	128.3	0.6	128.3	0.6
$C_{14}-C_{15}=C_{15'}$	123.0	123.8	0.8	123.8	0.8	123.6	0.6

[a] From ref 44. [b] Present work. [c] From ref 30.

effects of the conjugation on the optimized geometries. The confirmation that the stationary points reached in the calculations are true minima is made by performing vibrational calculations at the same level as those used in the optimization and checking that all the harmonic frequencies corresponding to the stationary point are real. These vibrational calculations also provide the theoretical IR and Raman spectra of the molecules.

The vibrational frequencies computed are, in general, larger than the experimental ones, due essentially to the fact that the theoretical treatments employed do not take into account the anharmonicity effects.[54] To calculate the anharmonic vibrational frequencies it is necessary to use the second-order perturbation theory, a method which is only applicable to molecules of small size,[55] or, alternatively, to correct the harmonic vibrational frequencies using scaling factors. The main difficulty of this second option is that there is no global universal scaling factor to apply to all molecules and methods. It is then necessary to compute the scaling factors for each theoretical method from the experimental and computed vibrational frequencies of a given number of small size molecules[54,56] and use them to account for the anharmonicity of larger size molecules. It has been shown that the overrating of the vibrational frequencies is in most cases uniform and that the harmonic vibrational frequencies can be properly corrected in this way.[57,54] The frequencies calculated in this work have therefore been corrected using the scale factors proposed in the literature for each level,[54,55,58,59] except for the stretching ν_{OH} frequencies for which the scale factors were 0.927 for capsanthin and 0.919 for capsorubin, chosen to fit the results to the experimental data.

All calculations were carried out using the Gaussian03 program package,[60] and the population analysis was made using the 3.1 version of the natural bond orbital (NBO) program implemented in this package.[61–63]

III. Numerical Results and Discussion

Geometry Optimization for β-Carotene. In Figure 1 we show the chemical structure of β-carotene[53] used as starting point

TABLE 6: Calculated Vibrational Frequencies (in cm^{-1}) for the Maxima of the Two Regions of the IR Absorption Spectrum and for the Absolute Maximum of the Raman Absorption Spectrum of β-Carotene ($\Delta\nu$ and $\Delta\nu_{scaled}$ Are the Differences between Calculated and Experimental Values before and after Frequency Scaling)

	IR spectrum											
	stretching C—C region				stretching C—H region				Raman spectrum			
method	ν	$\Delta\nu$	ν_{scaled}	$\Delta\nu_{scaled}$	ν	$\Delta\nu$	ν_{scaled}	$\Delta\nu_{scaled}$	ν	$\Delta\nu$	ν_{scaled}	$\Delta\nu_{scaled}$
HF/6-31G(d)	1115	145	998	28	3206	296	2870	−40	1852	328	1658	134
BLYP/6-31G(d)	1546	576	1536	566	2962	52	2944	34	1177	−347	1169	−355
BPW91/6-31G(d)[a]	1550	580	1488	518	3051	141	2929	19	1513	−11	1452	−72
SVWN/631G(d)	1663	693	1635	665	3057	147	3006	96	1176	−348	1156	−368
PBE0/631G(d)	1014	44	965	−5	3066	156	2918	8	1219	−305	1160	−364
B3LYP/6-31G(d)	1015	45	976	6	3043	133	2925	15	1581	57	1520	−4
B3LYP/6-31G(d,p)	1627	657	1564	594	3039	129	2921	11	1200	−324	1153	−371
B3LYP/6-311G(d)	1004	34	965	−5	3029	119	2912	2	1569	45	1508	−16
B3LYP/6-311G(d,p)	1004	34	971	1	3023	113	2925	15	1196	−328	1158	−366

[a] From ref 30.

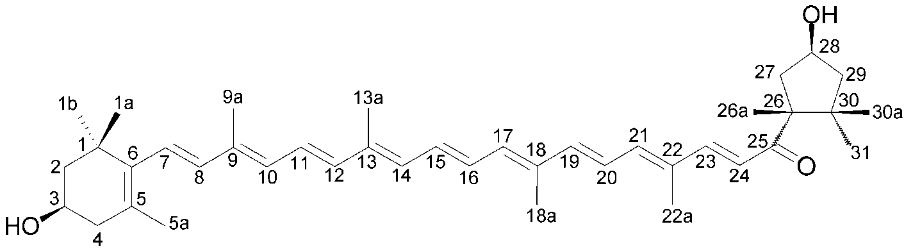

Figure 3. Molecular structure and atom numbering of capsanthin.

TABLE 7: Optimized Bond Lengths (in Ångstroms) and Wiberg Bond Indices of Capsanthin Calculated at the B3LYP/6-31G(d) Level

bond	length	Wiberg index	bond	length	Wiberg index
C_1-C_{1A}	1.548	0.9866	$C_{16}-C_{17}$	1.428	1.2361
C_1-C_{1B}	1.550	0.9893	$C_{17}=C_{18}$	1.375	1.5724
C_1-C_2	1.550	0.9825	$C_{18}-C_{18A}$	1.510	1.0235
C_1-C_6	1.546	0.9689	$C_{18}-C_{19}$	1.441	1.2011
C_2-C_3	1.523	0.9998	$C_{19}=C_{20}$	1.366	1.6206
C_3-O_3	1.430	0.9141	$C_{20}-C_{21}$	1.433	1.2163
C_3-C_4	1.529	0.9960	$C_{21}=C_{22}$	1.371	1.6033
C_4-C_5	1.514	1.0159	$C_{22}-C_{22A}$	1.509	1.0252
C_5-C_{5A}	1.511	1.0331	$C_{22}-C_{23}$	1.450	1.1696
$C_5=C_6$	1.356	1.7616	$C_{23}=C_{24}$	1.357	1.6912
C_6-C_7	1.475	1.0811	$C_{24}-C_{25}$	1.481	1.1008
$C_7=C_8$	1.355	1.7285	$C_{25}=O_{25}$	1.231	1.7210
C_8-C_9	1.454	1.1579	$C_{25}-C_{26}$	1.546	0.9573
C_9-C_{9A}	1.509	1.0255	$C_{26}-C_{26A}$	1.553	0.9825
$C_9=C_{10}$	1.369	1.6160	$C_{26}-C_{27}$	1.558	0.9797
$C_{10}-C_{11}$	1.434	1.2107	$C_{27}-C_{30}$	1.589	0.9484
$C_{11}=C_{12}$	1.365	1.6286	$C_{27}-C_{28}$	1.544	0.9907
$C_{12}-C_{13}$	1.442	1.1973	$C_{28}-O_{28}$	1.434	0.9206
$C_{13}-C_{13A}$	1.510	1.0242	$C_{28}-C_{29}$	1.544	0.9928
$C_{13}=C_{14}$	1.374	1.5748	$C_{29}-C_{30}$	1.549	0.9828
$C_{14}-C_{15}$	1.428	1.2359	$C_{30}-C_{30A}$	1.537	1.0025
$C_{15}=C_{16}$	1.369	1.6014	$C_{30}-C_{31}$	1.548	0.9956

TABLE 8: Optimized Bond Angles (in Degrees) of Capsanthin Calculated at the B3LYP/6-31G(d) Level

bond	angle	bond	angle
$C_1-C_2-C_3$	115.2	$C_{16}-C_{17}=C_{18}$	128.2
$C_2-C_3-C_4$	109.3	$C_{17}=C_{18}-C_{19}$	118.1
$C_3-C_4-C_5$	114.8	$C_{18a}-C_{18}-C_{19}$	118.5
$C_4-C_5=C_6$	122.7	$C_{18}-C_{19}=C_{20}$	126.7
$C_{5A}-C_5=C_6$	124.9	$C_{19}=C_{20}-C_{21}$	122.6
$C_1-C_6=C_5$	122.7	$C_{20}-C_{21}=C_{22}$	128.3
$C_5=C_6-C_7$	122.4	$C_{21}=C_{22}-C_{23}$	117.6
$C_6-C_7=C_8$	125.7	$C_{22a}-C_{22}-C_{23}$	118.7
$C_7=C_8-C_9$	126.4	$C_{22}-C_{23}=C_{24}$	125.6
$C_8-C_9=C_{10}$	118.1	$C_{23}=C_{24}-C_{25}$	129.7
$C_{9A}-C_9=C_{10}$	123.5	$C_{24}-C_{25}-C_{26}$	123.6
$C_9=C_{10}-C_{11}$	128.4	$C_{25}-C_{26}-C_{27}$	115.4
$C_{10}-C_{11}=C_{12}$	122.8	$C_{26a}-C_{26}-C_{27}$	109.2
$C_{11}=C_{12}-C_{13}$	126.7	$C_{26}-C_{27}-C_{28}$	107.0
$C_{12}-C_{13}=C_{14}$	118.2	$C_{27}-C_{28}-C_{29}$	105.8
$C_{13a}-C_{13}=C_{14}$	123.2	$C_{28}-C_{29}-C_{30}$	106.8
$C_{13}=C_{14}-C_{15}$	128.3	$C_{29}-C_{30}-C_{31}$	108.5
$C_{14}-C_{15}=C_{16}$	123.5	$C_{30a}-C_{30}-C_{31}$	108.4
$C_{15}=C_{16}-C_{17}$	123.4		

to carry out the optimization calculations of the geometry of this molecule. Although, as aforementioned, all the calculations were made without constraining the symmetry of the molecule, the equilibrium geometries obtained in all cases were shown to have a center of inversion located in the middle of the $C_{15}=C_{15'}$ bond, thus confirming that the molecule belongs to the C_i point group, as experimentally evidenced from the X-ray structure of the molecule[44] and from the IR and Raman spectra.[30,49] Accordingly, to describe the whole structure of β-carotene, it is sufficient to specify its geometrical parameters up to the 15′ carbon atom, as shown in Figure 1, since by symmetry the rest of the molecule is equivalent to its first half.

To determine the levels of theory that provide the best results for the equilibrium geometry of β-carotene, we have calculated the root mean square (rms) deviation of the bond distances and angles calculated at each level with respect to their experimental values available from the X-ray structure.[44] These deviations are listed in Table 1 and are split as observed into two columns, one for the distances and the other for the angles. Observation of this table shows first that of all the theoretical methods considered, the semiempirical AM1 is the one that provides the worst results for the geometrical parameters of the molecule of β-carotene, both for the bond lengths and the angles. It is also observed that the Hartree−Fock errors are in general larger than those from the density functionals, and these methods are therefore preferable for optimizing the geometry of β-carotene.

The proper comparison of the optimized structures calculated for β-carotene with the experimental X-ray structure requires

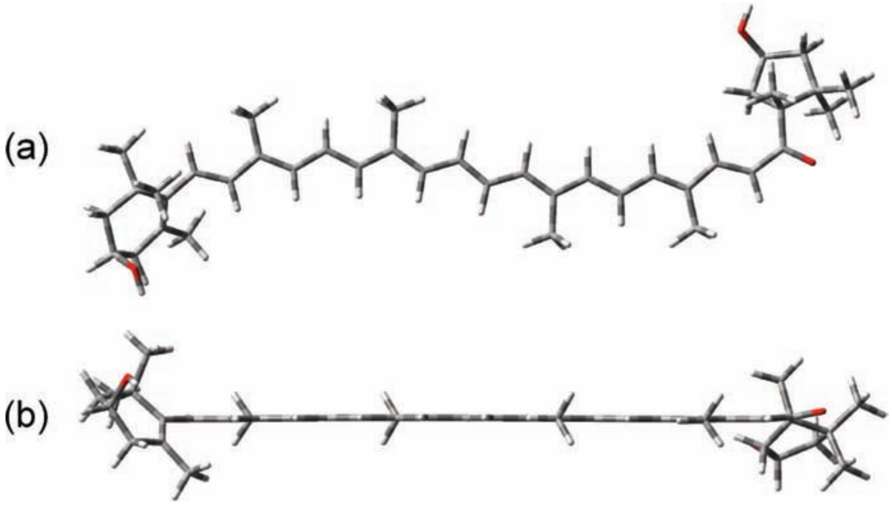

Figure 4. Molecular structure of capsanthin optimized at the B3LYP/6-31G(d) level. Normal (a) and lateral (b) views.

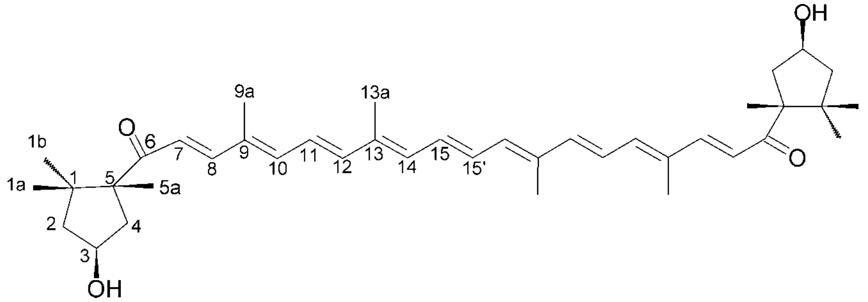

Figure 5. Molecular structure and atom numbering of capsorubin.

TABLE 9: Optimized Bond Lengths (in Ångstroms), Wiberg Bond Indices, and Angles (in Degrees) of Capsorubin Calculated at the B3LYP/6-31G(d) Level

bond	length	Wiberg index	bond	angle
C_1-C_{1A}	1.537	1.0027	$C_1-C_2-C_3$	106.8
C_1-C_{1B}	1.547	0.9959	$C_2-C_3-C_4$	105.8
C_1-C_2	1.549	0.9828	$C_3-C_4-C_5$	107.1
C_2-C_5	1.591	0.9472	$C_4-C_5-C_6$	115.5
C_2-C_3	1.544	0.9929	$C_{5A}-C_5-C_6$	105.7
C_3-O_3	1.433	0.9209	$C_5-C_6-C_7$	123.8
C_3-C_4	1.544	0.9907	$C_6-C_7=C_8$	129.6
C_4-C_5	1.558	0.9801	$C_7=C_8-C_9$	125.6
C_5-C_{5A}	1.552	0.9827	$C_8-C_9=C_{10}$	117.6
C_5-C_6	1.545	0.9578	$C_{9A}-C_9=C_{10}$	123.7
C_6-O_6	1.231	1.7253	$C_9-C_{10}-C_{11}$	128.2
C_6-C_7	1.482	1.0963	$C_{10}-C_{11}=C_{12}$	122.6
$C_7=C_8$	1.356	1.6973	$C_{11}=C_{12}-C_{13}$	126.6
C_8-C_9	1.451	1.1659	$C_{12}-C_{13}=C_{14}$	118.1
C_9-C_{9A}	1.508	1.0257	$C_{13A}-C_{13}-C_{14}$	123.4
$C_9=C_{10}$	1.370	1.6075	$C_{13}=C_{14}-C_{15}$	128.2
$C_{10}-C_{11}$	1.434	1.2134	$C_{14}-C_{15}=C_{15'}$	123.4
$C_{11}=C_{12}$	1.365	1.6253		
$C_{12}-C_{13}$	1.442	1.1980		
$C_{13}-C_{13A}$	1.510	1.0242		
$C_{13}=C_{14}$	1.374	1.5754		
$C_{14}-C_{15}$	1.428	1.2342		
$C_{15}=C_{15'}$	1.368	1.6040		

us to take into account the experimental standard deviations, which are 0.005−0.13 Å for the bond lengths and 0.3−0.5° for the bond angles.[44] Accordingly we see in Table 1 that, when the same 6-31G(d) basis set is used, the DFTs which provide the best results overall are the hybrid PBE0 and B3LYP functionals. Of these two functionals, B3LYP is the one which better reproduces the vibrational spectra of β-carotene, as will be shown below, so we have used this method to evaluate the effect of the size of basis sets on the results obtained. The basis sets used combine double and triple-ζ functions with polarization function over the heavy atoms and the hydrogen ones. The results of these calculations are also given in Table 1. When the p polar functions for the hydrogen atoms are included in the 6-31G(d) basis (6-31G(d,p) basis), we see that the errors for the bond distances and angles remain practically the same. The use of the triple-ζ 6-311G(d) and the 6-311G(d,p) bases does not improve the results either. The B3LYP/6-31G(d) level of calculation is then, presumably, the most appropriate for optimizing the geometry of β-carotene. In Figure 2, we depict the structure of the molecule optimized at this level.

To analyze in a more detailed way the effects of the electronic correlation on the optimization of the geometry of β-carotene, we give in Tables 2–5 the geometrical parameters calculated for this molecule at the AM1, HF/6-31G(d), SVWN/6-31G(d), PBE0/6-31G(d), BWP91/6-31G(d), BLYP/6-31G(d), and B3LYP/6-31G(d) levels. In these tables we also include the Δ differences between the theoretical and experimental values for the bond lengths and angles.

The Δ values for the bond lengths shown in Table 2 corresponding to the HF/6-31G(d) calculations indicate that this method makes a systematic error for the carbon−carbon distances in the conjugate system of the polyene chain. Specifically, the HF/6-31G(d) method gives longer single bond C−C distances and shorter double bond C=C distances than the experimental ones. This is due to the fact that the Hartree−Fock approach does not include the electronic correlation effects. The post-Hartree−Fock ab initio calculations based on configurations interaction or on perturbation theory, do indeed consider this correlation, but they are computationally out of reach for the large molecules studied here. The alternative

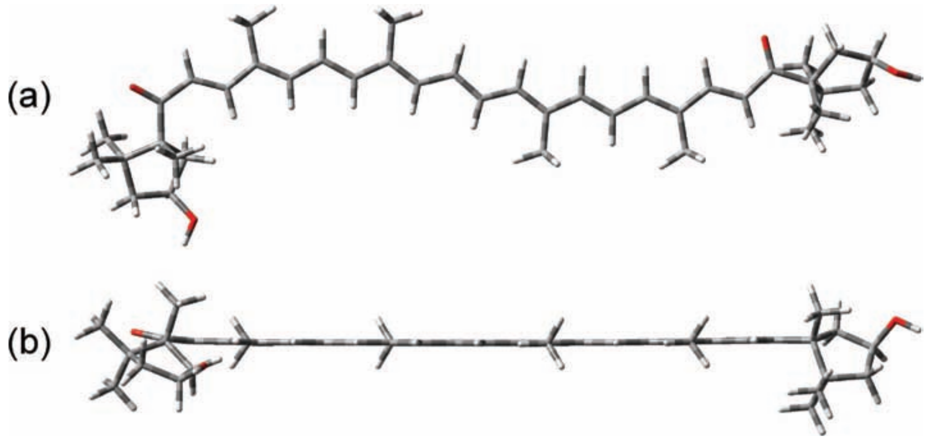

Figure 6. Molecular structure of capsorubin optimized at the B3LYP/6-31G(d) level. Normal (a) and lateral (b) views.

TABLE 10: Experimental and Corresponding Theoretical Frequencies (in cm^{-1}) of Bands in the IR Spectra of Capsanthin and Capsorubin[a]

capsanthin		capsorubin		
exptl[b]	theor	exptl[b]	theor	assignment[c]
	269(196)		301(196)	δ(O—H)
964vs	976(156)	961m	976(34)	δ(=C—H)$_{oop}$
		973m	983(231)	
1006s	998(373)	1006s	998(443)	$\delta(CH_3)_{rocking}$
1049vs	1060(563)	1051s	1068(1005)	$\Phi + \nu$(C—O)
	1090(275)	1106m	1089(454)	
1156m	1158(363)	1143m	1172(500)	ν(C—C)
1184m	1170(570)	1184m	1191(690)	
	1186(403)		1198(550)	
1254m	1235(415)	1251m	1234(650)	ν(C—C) + δ(O—H)
1319w	1272(204)	1283m	1270(262)	δ(=C—H)$_{ip}$
1365m	1375(183)	1368m	1361(98)	$\delta_s(CH_3)$
1397m	1387(145)	1375m	1375(188)	
	1399(132)	1388m	1392(238)	
1455m	1456(163)		1487(136)	$\delta_{as}(CH_3)$
1514m	1485(120)			
1553vs	1516(880)		1561(1377)	ν(C=C)
1578s	1563(316)		1600(576)	
1601w	1592(405)			
1664m	1643(500)	1665m	1646(934)	ν(C=O)
2867m	2927(410)	2873w	2932(350)	$\nu_s(CH_3,CH_2)$
2917s	2986(280)	2936m	2972(170)	$\nu_{as}(CH_3,CH_2)$
2956s	2970(150)	2958m	2988(285)	
3028w	3020(184)		3028(172)	ν(=C—H)
	3067(86)		3061(105)	
3329m	3329(14)	3433w	3433(21)	ν(O—H)

[a] The theoretical frequencies are calculated at the B3LYP/6-31G(d) level and properly scaled to account for anharmonicity (see text). The IR calculated intensities (in km/mol) are given in parentheses. [b] The intensities vs, s, m, and w correspond to 100−75, 75−50, 50−20, and 20−15% of absorption.[48] We have not considered weaker signals in the spectra, that is intensities <15%. [c] ν, stretch; δ, deformation; δ_{opp}, deformation out of the polyene chain plane; δ_{ip}, deformation in the polyene chain plane; Φ, ring deformation. The subscripts in the normal modes labeling denote their symmetry, with "s" standing for a symmetrical mode and "as" for a symmetrical or antisymmetrical mode depending on the molecule.

TABLE 11: Experimental and Corresponding Theoretical Frequencies (in cm^{-1}) of Bands in the Raman Spectra of Capsanthin and Capsorubin[a]

capsanthin		capsorubin		
exptl[b]	theor	exptl	theor	assignment[c]
1517	1516 (9.6×10^5)		1517 (8.7×10^5)	ν(C=C)
1157	1160 (3.3×10^5)		1173 (1.1×10^5)	ν(C—C)
1009	995 (7.4×10^4)		997 (8.8×10^4)	$\delta(CH_3)_{rocking}$

[a] The theoretical frequencies are calculated at the B3LYP/6-31G(d) level and properly scaled to account for anharmonicity (see text). The Raman scattering activities (Å^4 /amu) are given in parentheses. [b] Experimental frequencies from ref 49. [c] Vibrations: ν, stretch; δ, deformation.

then is to use DFT methods, which permit us to include the electronic correlation at a much lower computational cost. As can be observed in Tables 2 and 3, the Δ differences provided by the DFT methods do not follow the systematic error pattern of the HF/6-31G(d) calculation. Moreover, the Δ values obtained from the DFT calculations result in lower rms deviations for the geometric parameters of the molecule than those from the HF calculation, as previously shown in Table 1.

From the data included in Tables 2 and 3, it is also possible to extract information on the conjugated bond system of the β-carotene molecule. The interatomic distances for the carbon atoms in the initial geometry are 1.540 Å for single bonds and 1.355 Å for double bonds. After optimizing the geometry of the molecule, the interatomic distances calculated for the carbon atoms with indexes between 5 and 15′ lie in the range of 1.475−1.429 Å for single bonds and in the range of 1.369−1.358 Å for double bonds. The geometry optimization therefore leads to a shortening of the single bonds and to a lengthening of the double bonds, in accordance with the experimental data,[44] and confirms the conjugation existing in the polyene chain. It is also observed that the distance calculated for the C_6—C_7 bond is shorter than that expected for a nonconjugated single bond, while the distance calculated for the C_5=C_6 is longer than that for a nonconjugated double bond, regardless of the theoretical method employed. This result reveals the existence of a partial conjugation between the double bond of the terminal β-ionone ring and the rest of the chain. The value of the angle formed between the conjugated chain and the double bond of the terminal cyclic system, defined as C_5=C_6—C_7=C_8 and computed at the B3LYP/6-31G(d) level, is 47.2°. This value agrees with the experimental one of 42.5°[44] and coincides with the value obtained by Berezin et al.[31] at the same level of calculation.

To investigate further the conjugation in the β-carotene molecule, we have calculated the Wiberg bond indices (a measure of the bond order based on NBO analysis) for this molecule at the B3LYP/6-31G(d) level, the values of which are included in Table 3. As observed, the Wiberg indices for the C—C bonds outside the conjugated system take values between 1.0340 and 0.9661, while the index for the partially conjugated C_6—C_7 bond is 1.0813, and the indices for the C—C bonds in the polyene chain vary between 1.1560 and 1.2331. These results

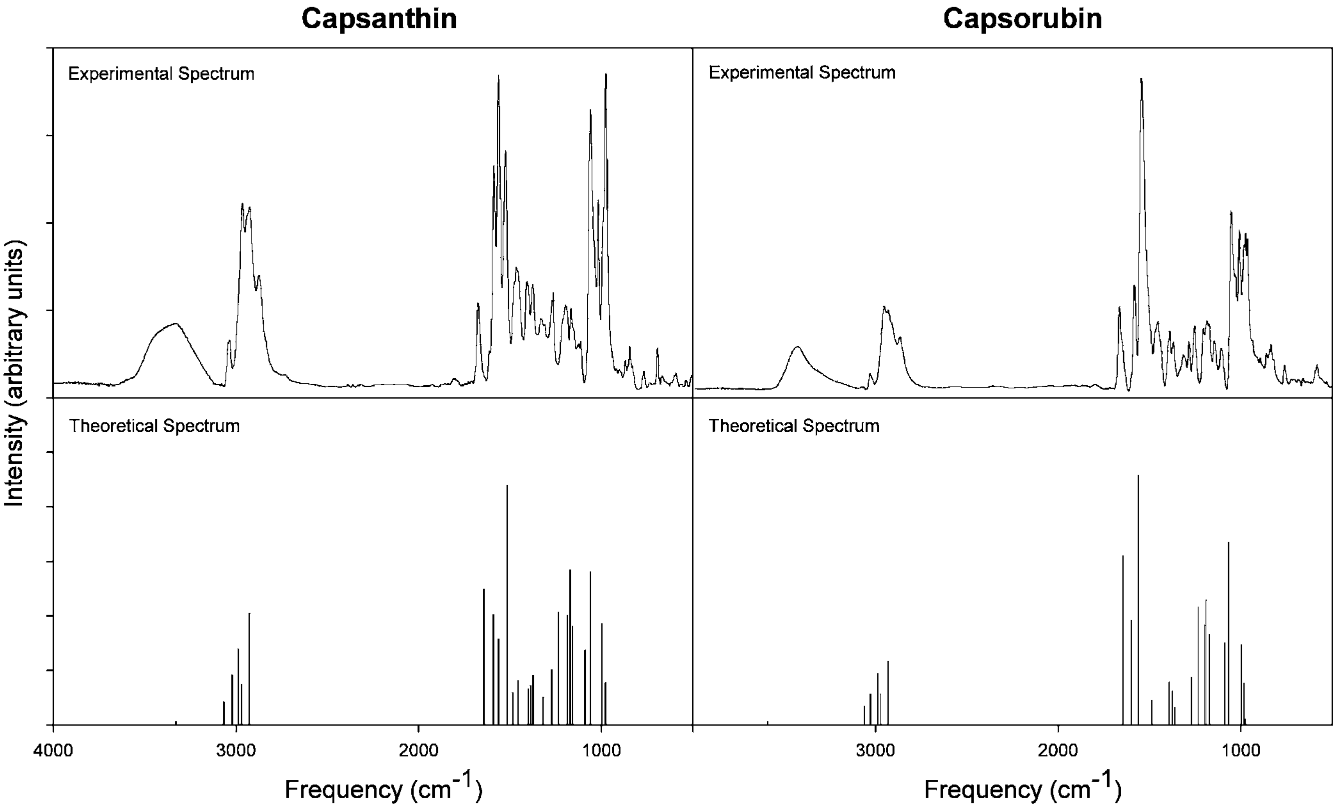

Figure 7. Comparion of the experimental (top) and theoretical (B3LYP/6-31G(d)) (bottom) vibrational IR spectra of capsanthin and capsorubin.

therefore agree with the shortening of the bond lengths previously discussed and confirm the conjugation in the polyene chain. It is also clearly seen that the conjugated system extends from the atoms 5 to 15′, with the $C_5{=}C_6{-}C_7$ bonds being only partially conjugated with the rest of the chain, due to the twist of 47.2°, and without the participation of the remaining *β*-ionone headgroup bonds.

It is thus made clear that the *β*-carotene molecule becomes stabilized by means of a twist of its terminal rings, as shown in Figure 2b where a lateral view of the optimized structure of the molecule is depicted. This spatial arrangement avoids the repulsion exerted by the hydrogen atoms of the methyl groups in the rings, on the hydrogen atoms situated at the ends of the polyene chain, despite the fact that this conformation involves a partial breaking of the conjugation of the double bond in the ring with the polyene chain. The twist of the terminal rings is not exclusive to carotenoids, since it had been observed earlier by Durbeej and Eriksson[64] to occur in the molecule of astaxanthin, whose chemical structure is very similar to that of *β*-carotene and where the twist angle of the terminal rings for the geometry optimized at the B3LYP/3-21G is of about 40°.

Calculation of the IR and Raman Spectra for *β*-Carotene. After optimizing the geometry of *β*-carotene, we have proceeded to calculate the IR and Raman vibrational spectra of this molecule and have checked again in this respect the efficiency of the different levels of calculation employed.

Experimentally, the IR spectra of carotenoids present two absorption regions, one located approximately between 1000 and 1600 cm^{-1}, which is mainly due to the stretching vibrations of the C—C bonds, and the other located about 3000 cm^{-1} where C—H stretching vibrations concentrate. For the molecule of *β*-carotene, absorption maxima are observed in each of these two regions at frequencies of 970 and 2910 cm^{-1}, respectively.[30] As far as the Raman spectra is concerned, carotenoids have two bands in the 1100−1200 and 1400−1600 cm^{-1} regions due to carbon—carbon single-bond and double-bond character, respectively.[65] For *β*-carotene in particular, the strongest intensity observed by Schulz and Baranska[49] is for C=C stretching at 1524 cm^{-1} . To analyze the ability of the different theoretical methods employed in this work to reproduce these experimental frequencies, we have calculated the frequencies of the two absorption maxima of the IR spectrum and the frequency of the strongest maximum of the Raman spectrum, and compared them with the corresponding experimental frequencies. We have excluded here the AM1 method due to the high rms that it provides for the bond lengths of the molecule.

In Table 6, we give the frequencies obtained for the spectra of *β*-carotene at the different levels of calculation and the $\Delta\nu$ differences with the experimental values both before and after proper scaling of the theoretical frequencies in order to take into account the anharmonicity effects.[54,55] We note first in Table 6 the very large errors that the BLYP/6-31G(d), BPW91/6-31G(d), SVWN/6-31G(d), and B3LYP/6-31G(d,p) methods give for the stretching C—C frequency of the IR spectrum, with $\Delta\nu$ values larger than 500 cm^{-1} both before and after scaling. Next we see that, in the Raman spectrum, the HF/6-31G(d), BLYP/6-31G(d), SVWN/6-31G(d), PBE0/6-31G(d), B3LYP/6-31G(d,p), and B3LYP/6-311G(d,p) methods all deviate by more than 300 cm^{-1} from the experimental frequency, again with or without frequency scaling. The differences between the calculated and the experimental IR stretching C—H frequencies are also large in general for all methods without scaling, but now all of them are reduced to a greater or lesser extent after scaling. The large deviations provided by these methods are due to the fact that the absorption maxima predicted by them do not coincide with the brightest experimentally observed signals, as already noted in previous studies on β-carotene.[30,31]

On considering the levels of calculations that provide the best results for the vibrational spectra of β-carotene, we see in Table 6 that of the two functionals that better reproduce the X-ray experimental geometry of the molecule, PBE0 and B3LYP, only the B3LYP functional with the 6-31G(d) and 6-311G(d) bases adequately describe both the IR and the Raman spectral profiles. In addition, the values of the frequencies calculated by these two methods significantly improve when scaled. However, as occurs in the geometry optimization calculations, the increase of the basis size does not improve the IR frequencies of the absorption maxima significantly and even slightly worsens the scaled Raman frequency. So the B3LYP/6-31G(d) method is the best option to choose, on account of its lower computational cost. The vibrational spectrum of β-carotene has already been calculated, and interpreted, at the B3LYP/6-31G(d) level by Berezin and Nechaev.[31] Our contribution in this respect has been therefore to give a proper justification for the choice of this level of calculation for the theoretical study of this type of molecules.

Geometry Optimization for Capsanthin and Capsorubin. There is to our knowledge only one theoretical study by Pérez-Gálvez[27] on the molecules of capsanthin and capsorubin where the delocalization of the charge along the polyene system is determined using a semiempirical treatment. We have therefore carried out the optimization of the geometries of these two molecules at the B3LYP/6-31G(d) level of calculation, which has been shown to work best to describe the structure and the vibrational spectra of β-carotene.

The initial basic structure of the capsanthin molecule does not have any symmetry element, as is shown in Figure 3. To describe the structure of this molecule completely it is therefore necessary to consider all its bond distances and angles. In Tables 7 and 8, we give the values of all the geometrical parameters of the molecule obtained after carrying out the B3LYP/6-31G(d) optimization, with the numbering of the atoms being as appears in Figure 3. We also include in Table 7 the Wiberg indices calculated at this level. As for β-carotene, the optimization of the geometry of capsanthin gives rise to a shortening of the single C—C bonds and an elongation of the double C═C bonds, thus making the conjugation of the polyene chain of this molecule clear. The Wiberg bond orders effectively confirm that the C—C bonds located between the carbon atoms 5 and 25 in the polyene chain form a conjugated system.

The optimized structure of the molecule of capsanthin is shown in Figure 4. It is observed first that the β-ionone ring is spatially oriented as forming an angle of 46.42° with respect to the polyene chain. This value is very close to that of 47.2° formed by the β-ionone rings in the molecule of β-carotene and obtained at the same level of calculation. Second, the angle $O_{25}{=}C_{25}{-}C_{24}{=}C_{23}$ between the carbonyl group and the last double bond of the polyene chain on the opposite side of the molecule has a value of 167.90°, with a bond $C_{25}{-}C_{24}$ length of 1.481 Å and a bond order of 1.1008. These values show that the carbonyl group is conjugated with the polyene chain, since the double C═O bond adopts a close-to-planar orientation relative to the chain and a shortening occurs in the bond $C_{25}{-}C_{24}$ length. The planarity of the double C═O bond is favored by the extension of the electronic conjugated system thus gained and by the fact that there is no steric stress to prevent such a spatial configuration, as in the β-carotene molecule.

The comparison of the geometry of capsanthin optimized at the B3LYP/6-31G(d) levels (Tables 7 and 8) with the geometry of β-carotene optimized at the same level (Tables 2 to 5) shows that the Wiberg indices and the bond distances and angles for both the polyene chain and the β-ionone terminal ring are practically identical in these two molecules. These results reveal therefore that the replacement of one of the β-ionone rings in the molecule of β-carotene by a substituted cyclopentene ring in the molecule of capsanthin leaves the structure of the rest of the molecule practically unaltered.

In the capsorubin molecule the polyene chain ends at both sides in carbonyl groups bonded to substituted cyclopentene rings, as shown in Figure 5. The optimization of the geometry of this molecule, performed as aforementioned with no symmetry constraints, reveals that this molecule has a C_2 symmetry axis perpendicular to the conjugated system plane located in the middle of the $C_{15}{-}C_{15'}$ bond. The capsorubin molecule belongs therefore to the C_2 symmetry point group, and it is sufficient to specify its geometry up to the 15′ carbon atom to characterize its whole structure.

The values of the Wiberg indices and the bond distances and angles for the molecule of capsorubin, optimized at the B3LYP/6-31G(d) level, are included in Table 9. These values make clear again the conjugation of the polyene chain, as evidenced by the decrease of the single bond C—C distances and the increase of the double bond C═C distances, and furthermore by the increase of the bond orders with respect to those of the bonds that do not form part of the conjugated system. Each of the double bonds of the carbonyl groups on both sides of the molecule is also conjugated with the polyene chain, with the $C_6{-}C_7$ bond length taking a value of 1.482 Å and a bond order of 1.0963, which are very close to those corresponding to the capsanthin molecule. This conjugation also reveals the almost planar orientation that the carbonyl groups tend to form with respect to the polyene chain, as seen in Figure 6, with a dihedral $O_6{=}C_6{-}C_7{=}C_8$ angle of 166.61°, which is very close to that calculated for the capsanthin molecule.

Calculation of the IR and Raman Spectra for Capsanthin and Capsorubin. Finally we have determined the IR and Raman spectra of capsanthin and capsorubin molecules also at the B3LYP/6-31G(d) level of calculation. The vibrational frequencies computed for these two molecules together with the experimental frequencies measured by Lorand et. al[48] for the IR spectra of the two molecules, and by Schluz and Baranska[49] for the Raman spectrum of capsanthin, are all included in Tables 10 and 11. As far as we know, there is no experimental Raman spectrum available in the literature for the capsorubin molecule. As for β-carotene, the calculated frequencies of capsanthin and capsorubin are corrected using the scale factor proposed by Scott and Radom[54] in order to account for the anharmonicity. In Tables 10 and 11 we also give the interpretation of the vibrational normal modes associated to the different bands of the two molecules. As can be seen, the theoretical IR and Raman spectra calculated for capsanthin and capsorubin reproduce the experimental frequencies of the main signals well, with it being possible to assign their corresponding vibrational normal modes even in relatively dense regions of the spectra. The good agreement between the calculated and experimentally IR observed spectra of the two molecules is better displayed in Figure 7, where these spectra are depicted comparatively.

IV. Conclusions

In this work we have studied first the ability of different theoretical methods, including semiempirical (AM1), Hartree–Fock, and a number of DFTs (SVWN, PBE0, BLYP, BPW91, and B3LYP) with different basis sets, to reproduce the equilibrium geometry and the IR and Raman spectra of the β-carotene molecule, reaching the conclusion that the B3LYP/6-31G(d) level of calculation provides overall the best results in both tasks.

In the second place, we have determined the equilibrium geometries and the IR and Raman spectra of the capsanthin and capsorubin molecules at the B3LYP/6-31G(d) level of calculations, based on the fact that the chemical structures of these two molecules are very similar to that of the β-carotene molecule. The equilibrium structure determined for capsanthin reveals that the double bond of the β-ionone ring lies outside the plane of the molecule, forming an angle of 46.42° with it. This twist, which is also observed in the terminal β-ionone rings of β-carotene, is due to the repulsion between the hydrogen atoms of the methyl groups bound to the ring and the hydrogen atoms of the polyene chain and gives rise to a partial lost of the conjugation of the β-ionone double bond with the rest of the molecule. At the other end of the polyene chain of capsanthin, the dihedral angle formed by the double bond of the carbonyl group with the last double bond of the chain takes a value of 167.90°. In this case there is no repulsion enforcing the C═O double bond to come out of the molecular plane, so the carbonyl group lies in a spatial orientation close to planarity, thus favoring the extension of the conjugated system. For the capsorubin molecule, which has a carbonyl group at both ends, the dihedral angle between the carbonyl double bond and the last double bond of the polyene chain has a value of 166.61°.

The results make it clear that when the headgroup of one carotenoid is a β-ionone ring, the double bond of the ring is partially conjugated with the rest of the polyene chain due to the twist of the ring to avoid the steric stress. However, when the polyene chain ends in a carbonyl group, there is no such stress and the double C═O bond tends to be situated in the plane of the molecule in order to extend the conjugate system and thus stabilize the molecule further. Our results also indicate that the changes of the headgroups at the end of the polyene chain do not significantly alter either the structure of the chain or that of the other headgroup.

Finally we have shown that the theoretical IR and Raman spectra calculated for the molecules of capsanthin and capsorubin at the B3LYP/6-31G(d) level are in good agreement with the experimental spectra, after proper scaling of the absorption frequencies to account for the anharmonicity contributions. This allowed us to assign the vibrational normal modes corresponding to the main bands of the experimental spectra of these molecules.

Acknowledgment. The work was partially supported by the Ministerio de Educación y Ciencia of Spain under Project CTQ2004-07818-CO2-01/BQU, by FEDER funds from the European Union, and by the Fundación Séneca del Centro de Coordinación de la Investigación de la Región de Murcia under Project 00508/PI/04. One of the authors (J.P.C.C.) acknowledges a fellowship provided by the Ministerio de Educación y Ciencia of Spain. The authors thank also Professor Lóránd for supplying the experimental IR spectra of the capsanthin and capsorubin molecules.

References and Notes

(1) Kull, D.; Pfander, H. *Carotenoids: Isolation and Analysis*; Birkhauser Publishing, 1995.

(2) Mortensen, A.; Skibsted, L. *J. Agric. Food Chem.* **1997**, *45*, 2970–2977.

(3) Martin, H.; Ruck, C.; Schmidt, M.; Sell, S.; Beutner, S.; Mayer, B.; Walsh, R. *Pure Appl. Chem.* **1999**, *71*, 2253–2262.

(4) Min, D.; Boff, J. *Comp. Rev. Food Sci. Food Safety* **2002**, *1*, 58–72.

(5) Montenegro, M.; Nazareno, M.; Duranti, E.; Borsarelli, C. *Photochem. Photobiol.* **2002**, *75*, 353–361.

(6) Stahl, W.; Sies, H. *Mol. Aspect Med.* **2003**, *24*, 345–351.

(7) El-Agamey, A.; Lowe, G.; McGarvey, D.; Mortensen, A.; Phillip, D.; Truscott, T.; Young, A. *Arch. Biochem. Biophys.* **2004**, *430*, 37–38.

(8) Krinsky, N.; Johnson, E. *Mol. Aspect Med.* **2005**, *26*, 459–516.

(9) Krinsky, N. *Nutrition* **2001**, *10*, 815–817.

(10) Omoni, A.; Aluko, R. *Trend Food Technol.* **2005**, *16*, 344–350.

(11) Nishino, H. *J. Cell. Biochem.* **1995**, *22*, 231–235.

(12) Mayne, S. *FASEB J.* **1996**, *10*, 690–701.

(13) Zeb, A.; Mehmood, S. *Pakistan J. Nutrition* **2004**, *3*, 199–204.

(14) Moore, J.; Hao, Z.; Zhou, K.; Luther, M.; Costa, J.; Yu, L. *J. Agric. Food. Chem* **2005**, *53*, 6649–6657.

(15) Mínguez-Mosquera, M.; Hornero-Méndez, D. *J. Agric. Food. Chem* **1993**, *41*, 1616–1620.

(16) Deli, J.; Matus, Z.; Tóth, G. *J. Agric. Food. Chem* **1996**, *44*, 711–716.

(17) Mínguez-Mosquera, M.; Pérez-Gálvez, A. *J. Agric. Food. Chem* **1998**, *46*, 5124–5127.

(18) Hornero-Méndez, D.; Mínguez-Mosquera, M. *J. Agric. Food. Chem* **2001**, *49*, 3584–3588.

(19) Minguéz-Mosquera, M.; Hornero-Méndez, D. *J. Agric. Food Chem.* **1994**, *42*, 640–644.

(20) Matsufuji, H.; Nakamura, H.; Chino, M.; Takeda, M. *J. Agric. Food Chem.* **1998**, *46*, 3468–3472.

(21) Pérez-Gálvez, A.; Mingéz-Mosquera, M. *J. Agric. Food Chem.* **2001**, *49*, 4864–4869.

(22) Maoka, T.; Mochida, K.; Kozuka, M.; Ito, Y.; Fujiwara, Y.; Hashimoto, K.; Enjo, F.; Ogata, M.; Nobukuni, Y.; Tokuda, H.; Nishino, J. *Cancer Lett.* **2001**, *172*, 103–109.

(23) Maoka, T.; Enjo, F.; Nishino, H. T. J. *FFI J.* **2004**, *209*, 3.

(24) Piekara-Saday, L.; Khaled, M.; Bradford, E.; Kispert, L. *Chem. Phys. Lett.* **1991**, *186*, 143–148.

(25) Connors, R.; Burns, D.; Farhoosh, R.; Frank, H. *J. Phys. Chem.* **1993**, *97*, 9351–9355.

(26) Woodall, A.; Lee, S.; Weesie, R.; Jackson, M.; Britton, G. *Biochim. Biophys. Acta* **1997**, *1336*, 33–42.

(27) Pérez-Gálvez, A.; Mínguez-Mosquera, M. *Biochim. Biophys. Acta* **2002**, *1569*, 31–34.

(28) Weesie, R.; Merlin, J.; Lugtenburg, J.; Britton, G.; Jasen, J. C. *Biospectroscopy* **1999**, *5*, 19–33.

(29) Himo, F. *J. Phys. Chem. A* **2001**, *105*, 7933–7937.

(30) Schlücker, S.; Szeghalmi, A.; Schmitt, M.; Poop, J.; Kiefer, W. *J. Raman Spectrosc.* **2003**, *34*, 413–419.

(31) Berezin, K.; Nechaev, V. *J. Appl. Spectrosc.* **2005**, *72*, 164–171.

(32) Gao, Y.; Focsan, A. L.; Kispert, L.; Dixon, D. *J.Phys. Chem. B* **2006**, *110*, 24750–24756.

(33) Dewar, M.; Zoebisch, E.; Healy, E.; Stewart, J. *J. Am. Chem. Soc.* **1985**, *107*, 3902–3909.

(34) Soffers, A.; Haandel, M. V.; Boersma, M.; Tyrakowska, B.; Laane, C.; Rietjens, I. *Free Rad. Res.* **1998**, *30*, 233–240.

(35) Stewart, J. *J. Comput. Chem.* **1989**, *10*, 209–220.

(36) Stewart, J. *J. Comput. Chem.* **1989**, *10*, 221–264.

(37) Kochk, W.; Holthausen, M. *A Chemist's Guide to Density Functional Theory*; Wiley-VCHWeinheim, 2001.

(38) Roothaan, C. *Rev. Mod. Phys.* **1951**, *23*, 69–89.

(39) Vosko, S.; Wilk, L.; Nusair, M. *Can. J. Phys.* **1980**, *58*, 1200–1211.

(40) Adamo, C.; Barone, V. *Chem. Phys. Lett.* **1998**, *298*, 113–119.

(41) Becke, A. *Phys. Rev. A* **1988**, *38*, 3098–3100.

(42) Lee, C.; Yang, W.; Parr, R. *Phys. Rev. B* **1988**, *37*, 785–789.

(43) Becke, A. *J. Chem. Phys.* **1993**, *98*, 5648–5652.

(44) Senge, M.; Hope, H.; Smith, K. *Z. Naturforsch.* **1992**, *C47*, 474–476.

(45) Vaswani, H.; Hsu, C.; Head-Gordon, M.; Fleming, G. *J. Phys. Chem. B* **2003**, *107*, 7940–7946.

(46) Spezia, R.; Zazza, C.; Palma, A.; Amadei, A.; Aschi, M. *J. Phys. Chem. A* **2004**, *108*, 6763–6770.

(47) Gaigeot, M.; Sprik, M. *J. Phys. Chem. B* **2004**, *108*, 7458–7467.

(48) Lóránd, T.; Deli, J.; Molnár, P.; Tóth, G. *Helv. Chim. Acta* **2002**, *85*, 1691–1696.

(49) Schuluz, H.; Baranska, M. *Vib. Spectrosc.* **2007**, *43*, 13–25.

(50) Balci, K.; Koch, A.; Kleinpeter, E. *J. Mol. Struct.* **2006**, *787*, 191–202.

(51) Dreuw, A.; Fleming, G.; Head-Gordon, M. *Phys. Chem. Chem. Phys.* **2003**, *5*, 3247–3256.

(52) Dokter, A.; van Hemert, M.; t Velt, C. I.; van der Hoef, K.; Lugtenburg, J.; Frank, H. *J. Phys. Chem. A* **2002**, *106*, 9463–9469.

(53) Deli, J.; Molnár, P. *Curr. Org. Chem.* **2002**, *6*, 1197–1219.

(54) Scott, A.; Radom, L. *J. Phys. Chem.* **1996**, *100*, 16502–16513.

(55) Andersson, M.; Uvdal, P. *J. Phys. Chem. A* **2005**, *109*, 2937–2941.

(56) Tantiringrotechai, Y.; Phanasant, K.; Roddecha, S.; Surawatanawong, P.; Sutthikhum, V.; Limtrakul, J. *THEOCHEM* **2006**, *760*, 189–192.

(57) Rauhut, G.; Pulay, P. *J. Phys. Chem.* **1995**, *99*, 3093–3100.

(58) Halls, M.; Velkovski, J.; Schlegel, H. *Theor. Chem. Acc.* **2001**, *105*, 413–421.

(59) Sinha, P.; Boesch, S.; Gu, C.; Wheeler, R.; Wilson, A. *J. Phys. Chem. A* **2004**, *108*, 9213–9217.

(60) Frisch, M. J.; Trucks, G. W.; Schlegel, H. B.; Scuseria, G. E.; Robb, M. A.; Cheeseman, J. R.; Montgomery, Jr., J. A.; Vreven, T.; Kudin, K. N.; Burant, J. C.; Millam, J. M.; Iyengar, S. S.; Tomasi, J.; Barone, V.; Mennucci, B.; Cossi, M.;. Scalmani, G.; Rega, N.; Petersson, G. A.; Nakatsuji, H.; Hada, M.; Ehara, M.;. Toyota, K.; Fukuda, R.; Hasegawa, J.; Ishida, M.; Nakajima, T.; Honda, Y.; Kitao, O.; Nakai, H.; Klene, M.; Li, X.; Knox, J. E.; Hratchian, H. P.; Cross, J. B.; Bakken, V.; Adamo, C.; Jaramillo, J.; Gomperts, R.; Stratmann, R. E.; Yazyev, O.; Austin, A. J.; Cammi, R.; Pomelli, C.; Ochterski, J. W.; Ayala, P. Y.; Morokuma, K.; Voth, G. A.; Salvador, P.; Dannenberg, J. J.; Zakrzewski, V. G.; Dapprich, S.; Daniels, A. D.; Strain, M. C.; Farkas, O.; Malick, D. K.; Rabuck, A. D.; Raghavachari, K.; Foresman, J. B.; Ortiz, J. V.; Cui, Q.; Baboul, A. G.; Clifford, S.; Cioslowski, J.; Stefanov, B. B.; Liu, G.; Liashenko, A.; Piskorz, P.; Komaromi, I.; Martin, R. L.; Fox, D. J.; Keith, T.; Al-Laham, M. A.; Peng, C. Y.; Nanayakkara, A.; Challacombe, M.; Gill, P. M. W.; Johnson, B.; Chen, W.; Wong, M. W.; Gonzalez, C.; Pople, J. A. *Gaussian 03*; Gaussian, Inc.: Wallingford, CT, 2004.

(61) Foster, J.; Weinhold, F. *J. Am. Chem. Soc.* **1980**, *102*, 7211–7218.

(62) Reed, A.; Weinstock, R.; Weinhold, F. *J. Chem. Phys.* **1985**, *83*, 735–746.

(63) Carpenter, J.; Weinhold, F. *THEOCHEM* **1988**, *169*, 41–62.

(64) Durbeej, B.; Eriksson, L. *Phys. Chem. Chem. Phys.* **2004**, *6*, 4190–4198.

(65) Withnall, R.; Chowdhry, B.; Silver, J.; Edwards, H.; de Oliveira, L. *Spectrochim. Acta A* **2003**, *59*, 2207–2212.

JP710304U